Naval Research Laboratory
Washington, DC 20375-5320

NRL/MR/6840--03-8673

A Review of the Development of Multiple-Beam Klystrons and TWTs

GREGORY S. NUSINOVICH

SAIC
McLean, VA

BARUCH LEVUSH
DAVID K. ABE

Vacuum Electronics Branch
Electronics Science and Technology Division

March 17, 2003

REPORT DOCUMENTATION PAGE

Form Approved
OMB No. 0704-0188

1. REPORT DATE *(DD-MM-YYYY)*	2. REPORT TYPE	3. DATES COVERED *(From - To)*
March 17, 2003	NRL Memorandum	2000 to 2002

4. TITLE AND SUBTITLE

A Review of the Development of Multiple-Beam Klystrons and TWTs

5a. CONTRACT NUMBER

5b. GRANT NUMBER

5c. PROGRAM ELEMENT NUMBER

6. AUTHOR(S)

Gregory S. Nusinovich,* Baruch Levush, and David K. Abe

5d. PROJECT NUMBER

5e. TASK NUMBER

5f. WORK UNIT NUMBER

7. PERFORMING ORGANIZATION NAME(S) AND ADDRESS(ES)

Naval Research Laboratory
4555 Overlook Avenue, SW
Washington, DC 20375-5320

8. PERFORMING ORGANIZATION REPORT NUMBER

NRL/MR/6840--03-8673

9. SPONSORING / MONITORING AGENCY NAME(S) AND ADDRESS(ES)

Naval Research Laboratory
4555 Overlook Avenue, SW
Washington, DC 20375-5320

10. SPONSOR / MONITOR'S ACRONYM(S)

11. SPONSOR / MONITOR'S REPORT NUMBER(S)

12. DISTRIBUTION / AVAILABILITY STATEMENT

Approved for public release; distribution is unlimited.

13. SUPPLEMENTARY NOTES

*SAIC, McLean, VA
(Permanent address: Institute for Research in Electronics and Applied Physics, University of Maryland, College Park, MD 20742

14. ABSTRACT

This memorandum summarizes the current (as of 2002) development status of microwave and millimeter-wave amplifiers based on multiple electron beam technology. A brief historical perspective of multiple-beam amplifier (MBA) research and development in the U.S. and abroad is presented covering the period from 1940 to 2002. Based on material gathered from conference and workshop presentations and recent open-literature journal publications, we summarize the current state-of-the-art in MBA device performance in Russia, France, and the Peoples' Republic of China. In addition, we develop a set of scaling analyses comparing multiple-beam klystron performance with single-beam klystron performance, including voltage, power, bandwidth, magnetic field, and dimensional scaling.

15. SUBJECT TERMS

Multi-beam; Multiple-beam; Multiple electron beam; Electron beam; Klystron; Amplifier; Vacuum electronics

16. SECURITY CLASSIFICATION OF:			17. LIMITATION OF ABSTRACT	18. NUMBER OF PAGES	19a. NAME OF RESPONSIBLE PERSON
a. REPORT	b. ABSTRACT	c. THIS PAGE			Baruch Levush
Unclassified	Unclassified	Unclassified	UL	50	19b. TELEPHONE NUMBER *(include area code)* (202) 767-0037

CONTENTS

1 INTRODUCTION

This memo is an attempt to summarize the current development status of amplifiers based on multiple electron beam technology. The material presented here has been collected from conference and workshop presentations, and from recent journal publications. In addition to reviewing the current state-of-the-art in device performance, we also present a set of scaling analyses comparing multiple-beam klystron (MBK) performance with a single-beam klystron (SBK) performance.

In preparing this work, we have benefited from technical discussions with Dr. Eduard Gelvich ("Istok," Russian Federation), Mr. Bill James (Communications and Power Industries, Palo Alto, CA), Dr. George Caryotakis (Stanford Linear Accelerator Center, Palo Alto, CA), Mr. Armand Staprans (Communications and Power Industries, Palo Alto, CA), and, in particular, Mr. Robert Symons (formerly of Litton Electron Devices, San Carlos, CA). While this memo cannot hope to cover all of the available material on multiple-beam amplifiers in depth, the authors hope that it presents a summary of current performance characteristics and provides a motivation for the further development of multiple-beam amplifiers in the U.S.

In Section 2, we begin with a brief history of the development of MBKs. Section 3 is devoted to derivations of basic performance dependencies on the number of parallel electron beams. In particular, this section provides insight as to the motivations for developing such amplifiers. Section 4 reviews some of these dependencies in the context of achievable power. In Section 5, the challenges that one encounters in the development of multiple-beam amplifiers are discussed and recent achievements in addressing these challenges are presented. In Section 6, the performance characteristics of different MBKs are presented in tabular form. In Section 7, a multiple-beam coupled-cavity TWT is described. And finally, Section 8 summarizes our observations regarding multiple-beam amplifiers.

2 HISTORY AND MOTIVATION

The single-beam klystron was invented by the Varian brothers in the late 1930s. Shortly afterwards (in the early 1940s) the multiple-beam klystron concept was introduced. The first series of MBK-relevant patents were submitted by V.F. Kovalenko in 1940 [1], J. Bernier in 1944 [2], and S.A. Zusmanovsky in 1955 [3]. At the time, MBK development was driven by the desire of microwave source developers to produce a given amount of microwave power at as low an operating voltage as possible (in general, lower voltages make power supplies simpler, lighter, cheaper, and more reliable).

However, in order to maintain a constant beam power, any reduction in the beam voltage must be accompanied by a corresponding increase in beam current. In conventional klystrons (as well as in many other microwave tubes), an increase in electron current density increases the role of space charge forces. At low current densities, these forces are negligibly small, and electrons that are initially modulated in the input cavity gap can ballistically bunch in the drift channels and be subsequently decelerated in the output cavity gap with high efficiency. At high current

Manuscript approved January 13, 2003.

densities, however, space charge forces are not negligible and repulsive forces between electrons interfere with the ballistic bunching, causing the bunches to lose coherence with a subsequent degradation in efficiency. In addition, high current densities require stronger magnetic fields for beam confinement, which can lead to higher system volume and weight.

Early on, it occurred to klystron designers that efficient operation with higher current beams could be achieved by separating the single electron beam into multiple beamlets, each with a sufficiently low current density to ensure efficient electron bunching. Each beamlet would be transported down its own individual drift channel, parallel to, but isolated from the other beamlets and allowed to interact only over small axial distances corresponding to cavity gap locations. Klystrons with such an electron beam generation and transport design have been termed "multiple-beam klystrons." Over the years, many multiple-beam klystron configurations have been considered [4]. A schematic of an MBK is shown in Fig. 1.

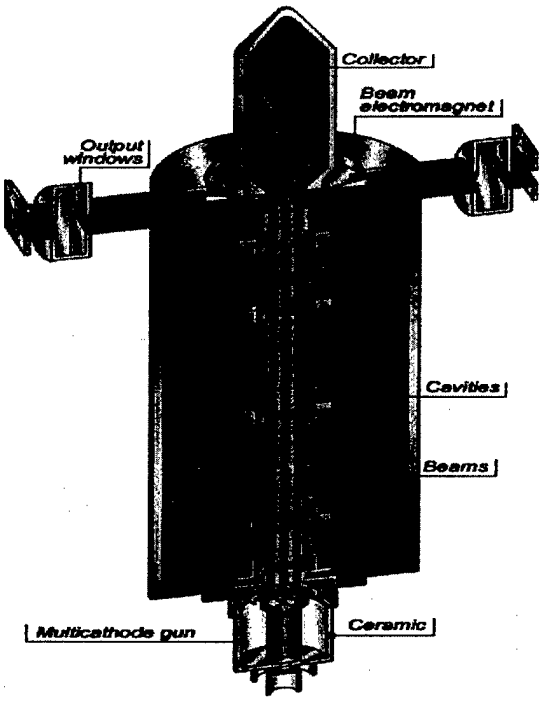

Figure 1: Schematic representation of a multiple-beam klystron (Thales Electron Devices, France [5]).

As one can see in the figure, electrons are emitted from multiple cathodes to form parallel beamlets that propagate through individual drift channels (metallic-walled tubes). At cavity locations, breaks are placed in the solid-walled tubes, allowing the beamlets to interact over the axial extent of the cavity gap. Once past the cavity, the beamlets re-enter their individual drift channels and propagate in isolation from one another.

Similar to single-beam klystrons, multiple-beam amplifiers can use both rf standing-wave and traveling-wave structures designed for operation in low-order (*e.g.*, fundamental) modes as well as in higher-order modes. The first MBK operating in a higher-order mode was designed and experimentally tested in the early 1960s by Boyd *et al.* [6].

The important advantage afforded by the MBK is a reduction in operating voltage relative to conventional SBKs, which leads to a more compact and lower-weight device. In addition to a reduction in operating voltage, another significant advantage of some multiple-beam device configurations is the potential for higher instantaneous bandwidths relative to SBKs. The bandwidth enhancement is a consequence of the presence of multiple beam tunnels. While the R/Q will be lower for the shorter, larger diameter gap necessary to accommodate the bundle of multiple beamlets, there will be a somewhat lower fraction of the electric field energy stored in the fringing fields around the gap, resulting in a lower gap capacitance and, consequently, a higher instantaneous bandwidth (see Section 3.4).

Despite some performance advantages of MBKs over SBKs, MBK development in the U.S. all but ceased after the early 1960s (see [7] for a summary of U.S. MBK research covering the period from the late 1950s through the 1960s). In part, the shift away from MBK research was due to the confidence and experience of U.S. engineers in high voltage design. At the time, there was a great strength in high voltage transmission line equipment design at Westinghouse, General Electric (GE), and many U.S. universities, in particular, Stanford University [8]. Also, Westinghouse and GE both had built early klystrons and klystron transmitters, and the experience of their engineers undoubtedly influenced decisions. Additionally, U.S. industry had achieved a high confidence in the design and manufacturing of single-beam convergent electron guns. The cessation of MBK work at GE occurred because GE was never able to provide a convincing solution to the off-axis convergent-beam focusing problems of their higher-order mode MBK approach [9]. Further development of competitive MBK designs would have required a considerable research and development investment in the fabrication and testing of numerous multiple-beam gun prototypes in the absence of effective computer-aided 3D electron gun design tools; at the time, it was felt that potential benefits of MBK technology did not outweigh the added device complexity and associated costs [10].

Over the past three decades, MBK research and development has occurred primarily in the former Soviet Union (FSU). Russian researchers have developed a wide variety of high-power MBKs in *L*-, *S*-, *C*-, *X*-, and K_u-bands using between 6 and 60 beams, with power gains from 40 to 45 dB, and electronic efficiencies in the range of 30% to 45%. Prior to the end of the Cold War, few details of these devices were published in the open literature as they were primarily developed for military applications.

The technology push behind the development of MBKs was a strong demand for communications systems and multi-function high-power radar systems, which could be satisfied only through the use of high-power, low-noise amplifiers. At the time that the FSU began its MBK development program, it was believed that the then-current state-of-the-art high-power, low-noise amplifiers (SBKs and traveling-wave tubes) were bulky, heavy, and required relatively high operating voltages. The large size and weight combined with the voltage requirements represented a significant drawback for applications in mobile, volume- and weight-constrained systems. To surmount these perceived drawbacks, FSU scientists and engineers focused significant

attention on the advantages of a multiple-beam approach, solving many scientific and technological problems along the way. (At the same time, SBK development was also actively pursued in the FSU and in other countries, resulting in significant progress over the past few decades in reducing the size and weight of single-beam devices).

The difference in the FSU and U.S. approaches to compact devices may, in part, be due to FSU technological advances in high-current-density cathodes that enable the production of the closely-spaced beamlets required in MBK designs. Alternatively, in the U.S., low-voltage crossed-field amplifier (CFA) technology got a significant boost. However, the main drawback of CFAs is their relatively high noise level.

At present, advances in computational tools for 3D electron gun design, combined with progress in cathode technology [11][12] and manufacturing techniques are providing a new impetus for MBK development in the U.S. For example, [12] reports a 10 A/cm^2 V-type reservoir cathode in continuous operation for in excess of 30,000 hours with very little degradation. Recently, a series of papers published in the open literature [13]-[19] have reported extraordinary performance characteristics of FSU-developed MBKs. These devices, which operate in a wide variety of frequency bands and peak/average powers, are currently being used in a number of defense, scientific, medical, and industrial applications. High-power MBKs are actively and successfully used in various types of radar, in communication and navigation systems, and for driving high energy charged particle accelerators. Medium-power MBKs are used in mobile radio-electronic systems, air-traffic control radar, and surveillance radar. Low-power miniaturized MBKs and multiple-beam coupled cavity traveling-wave tubes (CC-TWTs) are widely and successfully used in short-range radar and in low-weight navigation and communication systems.

In addition to the FSU, other countries have exhibited a growing interest in multiple-beam devices. Recently, France (Thales Electron Devices) has renewed its research and development activities in this area [20]. The People's Republic of China (PRC) also has a significant ongoing effort devoted to the development of a wide range of multiple-beam amplifiers [21]. The PRC's development program appears to be benefiting from a strong collaboration with Russian scientists [22][23]. Section 5 contains summaries of performance characteristics for a number of state-of-the-art multiple-beam devices.

3 MBK SCALING LAWS

In this section, we perform some basic analyses of multiple-beam klystron performance to develop scaling laws related to voltage, spatial dimensions, magnetic field strength and magnet weight, and bandwidth.

3.1 Voltage and Current Scaling

The reduction in voltage afforded by MBKs can be illustrated by comparing the cases of a multiple-beam klystron and a single-beam klystron generating the same level of radiating power under the following assumptions:

(i) the perveance of a single beamlet in the multiple-beam klystron is the same as the perveance of the entire beam in the single-beam klystron;

(ii) the power and efficiency of the multiple-beam and single-beam klystrons are identical;

(iii) the electron current density in both cases is limited by space charge effects.

Assume that the MBK consists of N independent and identical beamlets with current I_1 per beamlet. Then, the total microwave output power of such an MBK can be determined as,

$$P_{MBK} = N\eta I_1 V_{MBK} \tag{1}$$

where η is the efficiency of power extraction from each beamlet (since the beamlets are identical, their efficiencies are the same) and V_{MBK} is the beam voltage. Since we have assumed that space charge effects limit the electron current density, the dependence of I_1 on V_{MBK} is given by:

$$I_1 = (\mu P)_1 V_{MBK}^{3/2} , \tag{2}$$

where $(\mu P)_1$ is the perveance of a single beamlet. Substituting (2) into (1) yields,

$$P_{MBK} = N\eta (\mu P)_1 V_{MBK}^{5/2} . \tag{3}$$

Then, in accordance with the above assumptions, one can write,

$$P_{MBK} = P_{SBK} = \eta (\mu P)_1 V_{SBK}^{5/2} . \tag{4}$$

From (3) and (4) we can readily see that the voltages V_{MBK} and V_{SBK} are related as

$$V_{MBK} = \frac{V_{SBK}}{N^{2/5}} . \tag{5}$$

This is the scaling mentioned in [4]. The total beam current in MBKs is found by combining (1), (2), (4), and (5),

$$(I_b)_{MBK} = (I_b)_{SBK} N^{2/5} . \tag{6}$$

Obvious advantages of reducing the operating voltage include lower weight and volume of the tube and increased reliability. Additionally, since lower voltage beams produce less x-ray radiation at the collectors, the weight of collector radiation shields can be significantly reduced.

In the MBK, the total current, which scales in accordance with (6), consists of N beamlet currents, which we can represent either using the beamlet perveance as in (2) or using the beamlet electron current density,

$$\begin{aligned}(I_b)_{MBK} &= N I_1 \\ &= N(\mu P)_1 V_{MBK}^{3/2} \\ &= N (j_1)_{MBK} S_1\end{aligned} \tag{7}$$

where $(j_1)_{MBK}$ is the current density of a single MBK beamlet and S_1 is the corresponding cross-sectional area of the beamlet (note that we have implicitly assumed that the N beamlets are identical).

Similarly, the total current of a single-beam klystron can be written as,

$$\begin{aligned}(I_b)_{SBK} &= (\mu P)_1 V_{SBK}^{3/2} \\ &= j_{SBK} S_{SBK}\end{aligned} \tag{8}$$

where j_{SBK} is the current density of the single beam and S_{SBK} is the corresponding cross-sectional area of the single beam.

Dividing (7) by (8), we can relate the current density of a single MBK beamlet to the total single beam current density,

$$(j_1)_{MBK} = \frac{1}{N}\left[\frac{(I_b)_{MBK}}{(I_b)_{SBK}}\right]\left(\frac{S_{SBK}}{S_1}\right) j_{SBK} \tag{9}$$

If we further assume that the cross-sectional area of the beamlet is equal to the cross-sectional area of the total single beam ($S_1 = S_{SBK}$), then, using (6), the relation between the MBK and SBK current densities simplifies to,

$$(j_1)_{MBK} = \frac{j_{SBK}}{N^{3/5}} \ . \tag{10}$$

Alternatively, if we assume (*e.g.*, for the sake of transverse compactness) that the total cross-sectional area of all of the beamlets in the MBK is equal to the cross-sectional area of the single beam in the SBK ($NS_1 = S_{SBK}$), then we can write,

$$(j_1)_{MBK} = j_{SBK} N^{2/5}, \tag{11}$$

which is identical to the scaling found in [4].

3.2 Axial Length and Transverse Radius Scaling

The total axial length of the interaction region of any klystron is the sum of the lengths of the cavity gaps and the drift sections. In general, the length of each gap should be short enough to ensure that the transit angle through the gap, θ_g, is smaller than $\pi/2$ radians. The transit angle is defined as,

$$\theta_g = \frac{\omega L_g}{v_z} , \tag{12}$$

where ω is the frequency in radians/sec, L_g is the gap length, and v_z is the axial electron velocity. In gridless gaps, the transit angle through the gap is dependent on the degree to which the electric field penetrates into the drift tube on axis; this field penetration has the effect of increasing the effective length of the gap. As seen in (12), the gap length scales as the axial electron velocity, $L_g \propto v_z$. At non-relativistic voltages ($V_b << 511$ kV), v_z is proportional to the square root of the beam voltage, V_b, and thus,

$$L_g \propto V_b^{1/2} . \tag{13}$$

The lengths of the drift sections between the cavities are determined by the requirements for optimal beam bunching. For the simplest two-cavity configuration, the bunching parameter, q, which describes the ballistic bunching in the drift region, is given by,

$$q = \frac{\xi}{2} M \frac{\omega L_{dr}}{v_z} , \tag{14}$$

where $\xi = V_1/V_b$ is the modulation depth, that is, the ratio of the peak voltage, V_1 , across the modulating gap to the dc beam voltage, V_b; $M = \sin(\theta_g/2)/(\theta_g/2)$ is the gap coupling coefficient; and L_{dr} is the axial length of the drift section. The optimum value of the bunching parameter is $q_{opt} = 1.84$, which corresponds to the maximum of the Bessel function of the first order, which describes the ballistic bunching. If we assume that ξ and M are constant, then the lengths of drift sections follow the same scaling as the cavity gaps,

$$L_{dr} \propto v_z \propto V_b^{1/2} . \tag{15}$$

Therefore, the total length of the interaction region (gaps plus drift sections) should scale as the square root of the beam voltage and we see that a reduction in the beam voltage will lead to a reduction in the overall length of the device. Using this voltage scaling and (5), we can relate the total interaction length of an MBK, L_{MBK}, to that of a comparable single-beam device, L_{SBK} ,

$$L_{MBK} = \frac{L_{SBK}}{N^{1/5}} . \tag{16}$$

Note that, in order to localize the rf field inside the gap, the diameter of the drift channel, $2r_g$, should not exceed the axial length of the gridless gap, thus,

$$r_g \propto L_g \propto v_z \propto V_b^{1/2} . \tag{17}$$

This last scaling relies on our original assumption that the MBK and SBK efficiencies are identical. This is because the scaling relations of (15) and (17) preserve the gap-coupling coefficients, the plasma frequency, and the plasma frequency reduction factors [24].

Finally, as discussed in [14], we note that the favorable voltage and length scaling of the MBK yields a significant reduction in phase sensitivity to voltage fluctuations when compared with a TWT with the same gain.

3.3 Magnetic Field Scaling

The magnet system is the most difficult parameter for which to develop SBK-MBK scaling relations. The single- and multiple-beam geometries each have their own unique beam transport challenges that make it difficult to relate one system to another. In this section, we briefly describe some of the techniques for guiding single and multiple beams and develop some simple magnet weight-scaling relationships.

In an SBK, the magnetic field may or may not thread the cathode. In Brillouin-focused tubes, the field does not thread the cathode; alternatively, in tubes using what is often referred to as "convergent-confined-flow," it does. Usually, the axial magnetic field strength varies continuously along the beam. In Brillouin-flow tubes, electrons rotate around the axis. The field is increased toward the output end in order to keep the beam at a constant diameter, compensating for beam space charge effects that become increasingly significant as the charge density in the electron bunches builds up. In convergent-confined-flow tubes this technique is also used, but initially the flux in the beam contour is held fairly constant. The tapering of the field is accomplished by shaping iron pole-pieces and/or by changing the current in solenoid coils. The higher magnetic field at the output end of the tube is carefully adjusted to maximize efficiency.

In MBKs, one cannot increase the current in the coils that surround a group of beamlets or they will all converge toward the major axis of the tube. Perhaps one can shape the magnetic fields using iron around individual emitters, but typically, the cathode region of the MBK is not immersed in a magnetic field. Instead, the beamlets formed at the cathode face are electrostatically focused and pass through an iron pole-piece to enter their individual drift tubes. Downstream of the pole-piece, the beamlets are immersed in a guiding magnetic field. In the interaction region, this magnetic field is constant and axially-directed, but in the transition region around the pole-piece, the field has radial components as well. Thus, in the transition region, the beamlets acquire an angular velocity that causes a helical rotation about their individual axes. In order to accommodate the increased space charge forces in the higher-power output portions of the tube, the magnetic field must be stronger, the beamlet diameters smaller, and the gain lower than it would otherwise be in the low-level or input section of the tube. FSU scientists have developed an ingenious solution to this problem: they break the magnet up into several sections with pole-pieces having individual holes for each beamlet. In this arrangement, there is a stepwise increase in magnetic field at each pole-piece and the radial fields are symmetric about the axis of each individual beamlet. In higher-power, wideband MBKs with closely-spaced beamlets and emitters, it may be desirable to immerse the entire tube in a very strong magnetic field so that electrons will have to follow flux lines and the beam size will not change with local signal level.

The differences in the SBK and MBK magnetic field configurations required for good beam transport make it difficult to directly compare the weight and size of the respective magnet systems. However, with some assumptions, we can compare the weight of a magnet system that produces two to three times (maximum) the Brillouin field for comparable SBK and MBK devices.

To prevent electron interception on the drift tube walls, the beam electrons must be collimated and restricted to (primarily) axially-directed motion. In practice, this condition can be met when the axial magnetic field strength, B_z, is such that the cyclotron frequency, $\Omega = eB_z/m_e$, is several times larger than the electron plasma frequency, $\omega_p = \sqrt{m_e \rho / e\varepsilon_0}$, where ρ is the volume charge density and ε_0 is the permittivity of free space [25], or

$$B_z > \left(\frac{m_e \rho}{e \varepsilon_0} \right)^{1/2} . \tag{18}$$

We can write the volume charge density in terms of the electron number density, n,

$$\begin{aligned} \rho &= en \\ &= \frac{j}{v_z} , \end{aligned} \tag{19}$$

Substituting (19) into (18),

$$B_z > \left(\frac{m_e j}{e \varepsilon_0 v_z} \right)^{1/2} . \tag{20}$$

In the MBK, the beamlets propagate largely in isolation from each other. The short gap distances over which they interact are negligible from the standpoint of the guiding magnetic field and, therefore, the pertinent current density for use in (20) is the current density of a single beamlet, $(j_1)_{MBK}$. In the SBK case, the pertinent current density for use in (20) is the total beam current density, j_{SBK}. Assuming a weakly-relativistic beam, the axial magnetic field scaling inequality can be expressed as,

$$\frac{(B_z)_{MBK}}{(B_z)_{SBK}} > \left[\frac{(j_1)_{MBK}}{j_{SBK}} \right]^{1/2} \left(\frac{V_{SBK}}{V_{MBK}} \right)^{1/4} . \tag{21}$$

If we assume that the SBK and MBK have equal beam powers and that the perveance of a single MBK beamlet is equal to the perveance of the whole SBK beam, we can use the voltage scaling of (5) to write,

$$\frac{(B_z)_{MBK}}{(B_z)_{SBK}} > N^{1/10} \left[\frac{(j_1)_{MBK}}{j_{SBK}} \right]^{1/2} . \tag{22}$$

Finally, if we further assume that the cross-sectional area of the MBK beamlet is equal to the cross-sectional area of the total SBK single beam, we can use the current density scaling of (10),

$$\frac{(B_z)_{MBK}}{(B_z)_{SBK}} > N^{-1/5} \quad . \tag{23}$$

The optimization of the magnetic guiding system can have an enormous impact on minimizing the total system weight. As a rule, the magnet system is the dominant factor in the overall weight of a single- or multiple-beam klystron system, amounting to as much as four to ten times the combined weight of the gun, interaction circuit, and collector [19]. The particular advantage of the MBK configuration, which enables operation at a reduced voltage, is that the system weight (magnet and tube) can be decreased by a factor of ten or more in comparison with its single-beam counterpart [19]. This is because, as discussed in Section 3.2, the total electrodynamic interaction length of the MBK is shorter compared to an SBK of comparable output power. In addition, the perveance of each MBK beamlet is, in practice, smaller than the single beam of the SBK [in the limiting case, when the two perveances are equal, the voltage scaling is given by (5)]. Typically, the transverse dimensions of the SBK and MBK magnet systems are comparable, so the longitudinal dimension of the magnet system is the most important in regards to weight [26]. As the distance between the magnetic pole-pieces is proportional to the interaction length, the volume and weight of the magnets also scale with the interaction length. Thus, the magnet weight for the MBK system is decreased by the reduced field requirements described by (22) and (23), and also by the reduction in length as per (16).

Recent advances in high field, high coercivity, rare-earth materials for permanent magnets have enabled further weight and size reduction of MBKs. For example, light-weight (~ 5 kg) rare-earth periodic permanent magnet (PPM) focusing systems for MBKs have been developed at the Institute of Electronics, PRC. These magnets are manufactured from Nd-Fe-B and produce a 1-kG axially-directed magnetic field on the axis [27].

For permanent magnet systems, the magnet weight, w_m, can be estimated from [26],

$$w_m = \frac{B_z^2 l_m S_m}{(BH)_{\max}} \quad , \tag{24}$$

where B_z is the required on-axis axial magnetic field; l_m and S_m are the length and cross-sectional area of the magnetic system, respectively; and $(BH)_{\max}$, the magnetic energy product, is a measure of the maximum energy density that can be stored in the material and is a characteristic of the particular magnetic material.

To develop a permanent magnet weight scaling, we assume the following: the cross-sectional area of the MBK and SBK magnet systems are equal; the SBK and MBK have comparable beam power; the single MBK beamlet perveance is equal to the SBK beam perveance; and the cross-sectional area of the MBK beamlet is equal to the cross-sectional area of the total SBK single beam. Then, using the magnetic field scaling of (23) and the length scaling of (16), we can write,

$$\frac{(w_m)_{MBK}}{(w_m)_{SBK}} \propto N^{-3/5} \quad . \tag{25}$$

In practice, the diameter of the MBK tends to be larger than that of an SBK of comparable power and the corresponding magnet system tends to have a slightly larger cross-sectional area.

This fact has prompted Korolev [26] to propose a qualitative magnet system weight scaling of $N^{-1/2}$, which is quite close to (25).

Low power, miniaturized MBKs have been produced with much lower system weights. For example, a miniaturized K_u-band MBK developed at "Istok" delivers 400 W peak power with a duty cycle of ~30% and has a total weight (including the magnet) of only 400 g [19]. This device has a record average-power-to-weight ratio of ~ 0.3 Watts/g.

3.4 Bandwidth scaling

MBK bandwidth scaling was recently discussed in [29] and [30]. This scaling is based on the standard assumption that the bandwidth of a multiple-cavity klystron is limited by the bandwidth of its output cavity, which can be determined as

$$\begin{aligned} \frac{\Delta f}{f} &= \frac{1}{Q_L} \\ &= M^2 \rho_i \left(\frac{I_b}{V_b} \right) \end{aligned} \quad . \tag{26}$$

Here Q_L is the loaded Q-factor of the output cavity; M is the previously discussed interaction coefficient, which accounts for a finite electron transit angle in the cavity gap; $\rho_i = \sqrt{L/C}$ is the wave impedance (L is the equivalent inductance of the cavity and C is the total equivalent capacitance); and V_b and I_b are the cathode voltage and total beam current, respectively.

Using (26), for the SBK we can write

$$\left(\frac{\Delta f}{f} \right)_{SBK} = M^2 \rho_{i,SBK} \left[\frac{(I_b)_{SBK}}{V_{SBK}} \right] . \tag{27}$$

Similarly, for the MBK,

$$\left(\frac{\Delta f}{f} \right)_{MBK} = M^2 \rho_{i,MBK} \left[\frac{(I_b)_{MBK}}{V_{MBK}} \right] . \tag{28}$$

As in Section 3.1, we assume space-charge limited flow; the MBK and SBK beam powers are equivalent; and the MBK beamlet perveance equals the single beam perveance. Then, dividing (28) by (27), we can use (5) and (6) to write,

$$\frac{(\Delta f / f)_{MBK}}{(\Delta f / f)_{SBK}} = N^{4/5} \left(\frac{\rho_{i,MBK}}{\rho_{i,SBK}} \right) , \tag{29}$$

which suggests that if we make the MBK cavity wave impedance comparable to the SBK cavity wave impedance the MBK bandwidth will be enhanced proportional to $N^{4/5}$.

A more accurate evaluation of the scaling requires an analysis of the dependence of the wave impedance on the number of beams, N. We employ the standard method described in [31]. Consider a toroidal cavity, as shown schematically in Fig.2.

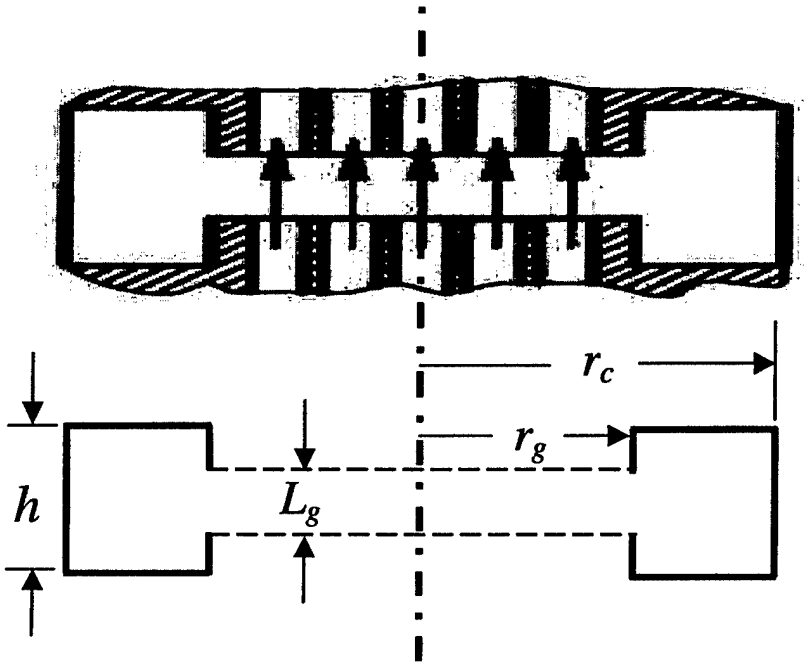

Figure 2: Schematic of a toroidal klystron cavity.

The total capacitance can be treated as the sum of the gap and cavity capacitances connected in parallel, $C = C_{gap} + C_{cav}$. In [32], the capacitances are shown to have the following dimensional dependencies,

$$C_{gap} \propto \frac{r_g^2}{L_g} \tag{30}$$

and

$$C_{cav} \propto r_g \, \ell n\left(\frac{h}{L_g}\right) \qquad for\ h \le 2(r_c - r_g)$$
$$, \tag{31}$$
$$C_{cav} \propto r_g \, \ell n\left[\frac{2(r_c - r_g)}{L_g}\right] \quad for\ h \ge 2(r_c - r_g)$$

where r_g is the radius of the inner wall of the cavity; r_c is the radius of the outer wall of the cavity; L_g is the axial extent of the cavity gap; and h is the height of the cavity. As discussed at the beginning of Section 3.2, in the gridless cavity the electric field penetrates into the drift tube on-

axis, increasing the effective length of the gap. However, when all dimensions are scaled proportionally, this effect does not change the scaling relations developed below.

If we assume that the total beam area scales as N, then the cavity inner wall radius scales as

$$r_g \propto N^{1/2} . \tag{32}$$

If we further assume that (h/L_g) and/or $(r_c\text{-}r_g)/L_g$ are constant with respect to the number of beamlets, then, from (31), it follows that

$$C_{cav} \propto r_g \propto N^{1/2}. \tag{33}$$

From (5) and (17), the axial extent of the gap scales as $L_g \propto \frac{1}{N^{1/5}}$. Substituting into (30),

$$C_{gap} \propto N^{6/5}. \tag{34}$$

Combining (33) and (34), we see that the total capacitance scaling with N has the form

$$C = AN^{6/5} + BN^{1/2} \tag{35}$$

where A and B are constants.

In [31], the equivalent inductance of the cavity, L, is shown to be,

$$L \propto h\, \ell n\left(\frac{r_c}{r_g}\right). \tag{36}$$

Assuming that r_c/r_g is constant with respect to the number of beamlets, we can again use (5) and (17) to show that the inductance scales as,

$$L \propto h \propto L_g \propto \frac{1}{N^{1/5}}. \tag{37}$$

Therefore, using (35) and (37), the wave impedance $\rho_i = \sqrt{L/C}$ scales as,

$$\rho_i \propto \frac{1}{N^{7/20}\sqrt{N^{7/10} + B/A}} . \tag{38}$$

Substituting this scaling into (29) yields a bandwidth scaling of

$$\left(\frac{\Delta f}{f}\right)_{MBK} \propto \frac{N^{9/20}}{\sqrt{N^{7/10} + B/A}}\left(\frac{\Delta f}{f}\right)_{SBK} . \tag{39}$$

We can consider two limiting cases for the denominator of (39). When $B/A << N^{7/10}$, (39) reduces to a rather weak function of the number of beamlets, $(\Delta f/f)_{MBK} \propto N^{1/10}$. On the other hand, when $B/A >> N^{7/10}$, the scaling dependence is much stronger, $(\Delta f/f)_{MBK} \propto N^{9/20}$. In the former case, for example, the bandwidth enhancement is about a factor of 1.4 for $N = 36$. This is consistent with the explanation that has been put forward in [4] for the MBK: as the number of beams increases, the decrease in the characteristic impedance of the cavity (inversely propor-

tional to C_{gap}) is weaker than the increase in beam conductance (I_b / V_b). In other words, the current increases with the area and the number of beams, but the capacitance of the fringing electric field around the interaction gaps only increases as the circumference of the bundle [4]. Therefore, the MBK achieves enhanced bandwidth at low voltage by maximizing the gap capacitance relative to the total cavity capacitance. In the limiting case, where we assume that the cavity capacitance is zero and that only the gap capacitance contributes to the wave impedance, the fractional bandwidth of the MBK would be about 0.24 times the microperveance of a single MBK beamlet [33].

In [4], an additional bandwidth scaling law is mentioned. It is based on the assumption that the total cross-sectional area of the individual beamlet drift tubes in an MBK is equivalent to the cross-sectional area of the drift tube of an SBK of comparable beam power (as in the preceding developments, the assumptions of space-charge limited flow and equality of beamlet and single-beam perveances still apply). In this case the drift tube radius, r_g, does not depend on N, and therefore the scaling for the total capacitance has the form,

$$C = A_1 N^{1/5} + B_1 \ , \tag{40}$$

where A_1 and B_1 have different values than the constants in (35). Using (40), the definition of the wave impedance, and assuming that the cavity inductance still scales as in (37), we again use (29) to develop a bandwidth scaling,

$$\left(\frac{\Delta f}{f}\right)_{MBK} \propto \frac{N^{7/10}}{\sqrt{N^{1/5} + B_1 / A_1}} \left(\frac{\Delta f}{f}\right)_{SBK} . \tag{41}$$

Once again, we can consider two limiting cases: for $B_1 / A_1 << N^{1/5}$, $(\Delta f / f)_{MBK} \propto N^{6/10}$; and for $B_1 / A_1 >> N^{1/5}$, $(\Delta f / f)_{MBK} \propto N^{7/10}$. In the former case, again using a 36-beam example, the bandwidth enhancement is about a factor of eight, which is consistent with [4].

Obviously, the required current density at the cathode for a tightly packed MBK will be very high. For example, according to [30], using a beamlet cathode current density of j = 15 A/cm^2, it is possible to achieve 28% bandwidth at a beam voltage of 24 kV and 20% bandwidth at 34 kV. For further bandwidth enhancement, MBK designers use techniques developed for single-beam klystrons, such as multi-gap resonators and the staggered-tuning of multiple-cavity circuits. However, at the higher frequencies (beginning at *X*-band and above, according to [15]), the MBK bandwidth does not follow the scaling developed in this section, as other constraints begin to dominate.

4 MBK POWER LIMITATIONS

As discussed in [30], it is convenient to express the scaling for the power handling capabilities of MBKs in terms of the available electron beam power, P_0. There are four critical parameters that can limit the beam power in an MBK: practical limits on the total beam perveance, $(\mu P)_N$; practical limits on the individual cathode emitter current density, j_c ; the maximum allowable electric field strength in the region between the cathode and the grid, E_{cg} ; and the maximum allowable electric field strength in the region between the grid and the anode, E_{ga}. The dependence of the beam power on these quantities has been developed in [30]:

$$P_0 = (\mu P)_N V_N^{5/2} \tag{42}$$

$$P_0 = j_c S_c N V_N \tag{43}$$

$$P_0 = F\lambda^{3/2} N^{1/4} E_{cg} E_{ga}^{1/2} V_N \tag{44}$$

where V_N is the MBK cathode voltage; S_c is the area of an individual cathode emitter; λ is the operating wavelength in free space; and the coefficient, F, depends on the geometry of the electron gun and on the ratio of the cathode voltage to the cutoff voltage.

Neglecting fringing, we can write the electric field strengths in the cathode-grid and grid-anode regions as,

$$E_{cg} = \frac{V_{co}}{d_{cg}} , \tag{45}$$

and

$$E_{ga} = \frac{(V_{co} + V_N)}{d_{ga}} , \tag{46}$$

where V_{co} is the current-cutoff grid voltage; and d_{cg} and d_{ga} are the cathode-grid and grid-anode spacings, respectively.

The coefficient, F, in (44) can be expressed as [30],

$$F = \frac{0.556\, K_3^{3/2} K_2^{3/4}}{(1+\delta/d_{cg})(1+V_{co}/V_N)^{1/2}} , \tag{47}$$

where δ is the thickness of the focus electrode (see Fig. 3).

Using (43), (45), (46), and (47), we can rewrite (44) as,

$$P_0 = j_c K_1 K_2 (\pi/4)(K_3\lambda)^2 V_N , \tag{48}$$

where $K_1 = S_c / S_{ch}$ is the ratio of the individual cathode emitter area, S_c, to the cross-sectional area of a single drift channel, S_{ch} ; $K_2 = N S_{ch} / S_{cl}$ is the ratio of the total area of the drift channels, $N S_{ch}$, to the area of the post, S_{cl} (alternatively called the "capacity lug", see Fig. 3); and K_3

$= D_{cl}/\lambda$ is the ratio of the diameter of this post (capacity lug) to the wavelength. In Fig. 3, these dimensional quantities are clearly marked for clarity.

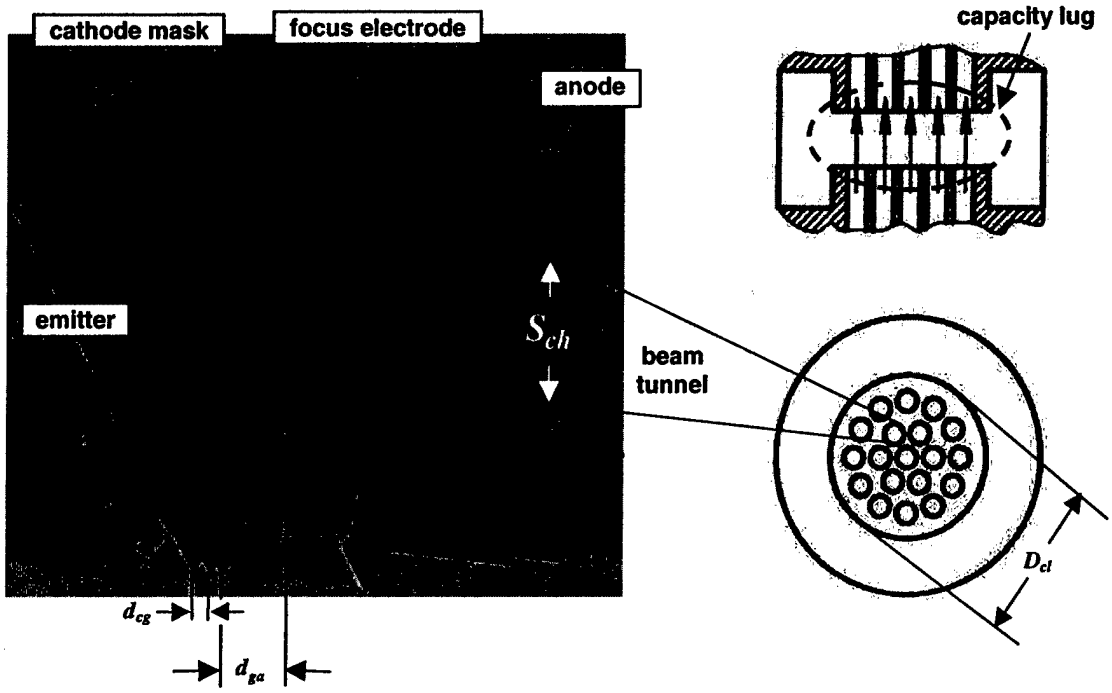

Figure 3: Schematic of a MBK gun and fundamental mode cavity [34].

MBKs with instantaneous bandwidths in the range of 2% to 10% have demonstrated electronic efficiencies on the order of 35% to 45% in *L*-, *S*- and *C*-bands, and 25% to 35% in *X*- and K_u-bands. Using these efficiencies and (48), one can convert beam power into an estimate of radiated output power. Note that, for low-convergence guns (beam-area compression ≤ 2, see Section 5.1) typical of multiple-beam devices, $K_1 \sim 1$, and, for high-power MBKs, $K_2 \sim K_3 \sim 0.5$.

Figures 4 and 5 plot some of the results of an analysis of the dependencies of (42)-(48) given in [30]. In Fig. 4, the beam power, P_0 , cathode current density, j_c , and total beam microperveance are plotted, using (48), as functions of wavelength for a 28-beam MBK operating at 34 kV with $K_1 = 1$ and $K_2 = K_3 = 0.5$. The maximum emitter current density is assumed to be 15 A/cm^2. At long wavelengths ($f < 4$ GHz) the beam power and total microperveance are independent of λ ($P_0 = 2.1$ MW and $(\mu P)_N = 10$), while at shorter wavelengths ($f > 4$ GHz), the beam power and total microperveance decrease with decreasing wavelength. Below 5 GHz, the cathode current density decreases with increasing wavelength. Above 5 GHz, the cathode operates at the maximum current density.

As a specific example, let us assume that our operating wavelength is 10 cm. Then, from Fig. 4, the total beam microperveance is about 10 with a corresponding total beam current of about 62.7 A. We have already assumed $N = 28$ beams, so each emitter produces ~2.2 A. If we further assume that the emitter area is $S_c = 0.35$ cm^2, then the single emitter current density is $j_c \approx 6.3$ A/cm^2.

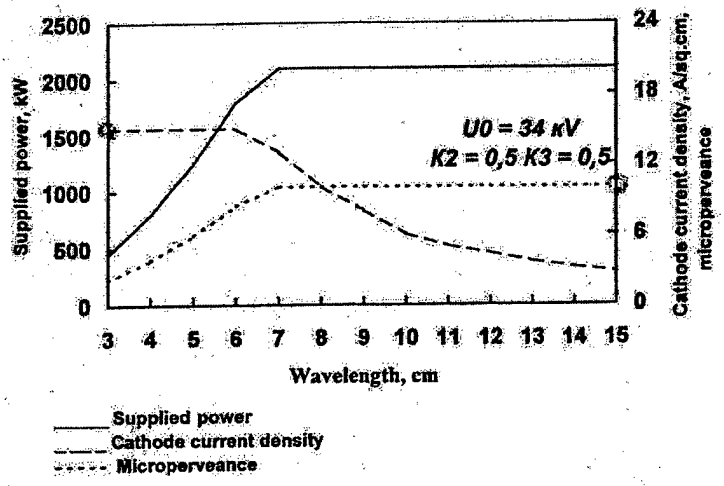

Figure 4: Power, current density, and microperveance as functions of wavelength [30].

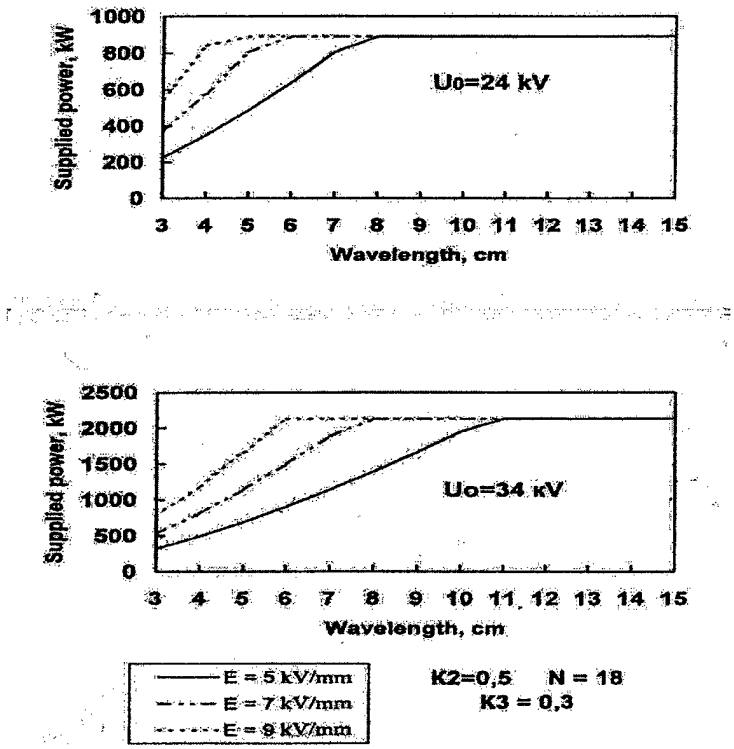

Figure 5: Maximum power versus wavelength for different values of the electric field between the cathode and the focus electrode [30].

Similar dependencies of the maximum supplied power on the wavelength are shown in Fig. 5 for several values of the electric field strength (E_{cg}=E_{ga}=E) and for two different operating voltages (24 kV and 34 kV). As seen in Fig. 5, at higher voltages the limitations on the power start at longer wavelengths. The practical limits for the electric field strengths, E_{cg} and E_{ga}, which signal the onset of breakdown in the gun region are in the range of 50-90 kV/cm [30]. Moreover, it is believed, based on current practices, the maximum value of the average output power of the MBKs using toroidal cavities operating in the fundamental mode is about 20 kW at λ ~7-15 cm and about 5 kW at λ ~3-4 cm [30].

5 MBK DEVELOPMENT ISSUES

The SBK and the MBK are based on the same physical principles. Of the two devices, however, the development of an MBK is more challenging as practically every major component is subject to more stringent requirements compared to the SBK: the cathode loading is higher; the magnetic and microwave circuits must be more highly optimized to achieve a desired level of performance; and manufacturing tolerances are more stringent. For example, in order to achieve 98% to 99% beam transmission in an MBK, the mutual alignments of the drift channels must be on the order of 0.02 to 0.1 mm and their overall alignment with the multiple-beam gun must be on the order of 0.4 mm to a few millimeters [14]. Beam transport requirements also place stringent demands on the uniformity of the magnetic field across the beamlets. All these issues notwithstanding, many types of MBKs have been successfully developed in Russia, France, and the PRC.

5.1 Cathode Loading, Electron Optics, and Collectors

Significant research and development effort has been focused on developing electron gun designs capable of producing N beamlets with near-laminar flow [4]. Since MBK beamlets must be closely packed to maximize gap filling, it is difficult to achieve high beam-area compression in the region between the cathode and the interaction space. Typically, in MBKs, the beam-area compression factor (the ratio of the cross-sectional area of the beam at the cathode to the cross-sectional area of the beam in the interaction region) is less than or equal to 2. This low compression ratio leads to high cathode loading requirements. (Historical note: multiple-beam guns with higher compression factors were demonstrated in the FSU in the 1980s, but were not used in production because of higher cost; eventually, advances in long-life, high current density cathodes made them unnecessary [18]). Recently, efforts have been undertaken in the U.S. to develop electron guns with multiple convergent beams [35]; this work is currently in progress.

Cathode technology is one of the most challenging sub-components of MBKs, particularly for those devices that operate in the fundamental mode. The critical issues for multiple-beam guns are similar to single-beam guns: alignment precision, emission uniformity, and lifetime versus current density. Obviously, it is more difficult to achieve precise alignment at high temperatures when you have multiple emitters, especially if shadow and control grids are used. The same is true for the case of uniform emission. But over the years, these problems have been successfully overcome.

At present, the main challenge for MBK cathode technology is the development of high current density emitters with long operational lifetimes. The current density requirements for a single beamlet emitter range from about 10 A/cm^2 to as much as 40 A/cm^2, depending on the device power and frequency. For example, [18] states that in the short-wavelength part of the centimeter-wave band, the cathode loading requirement reaches > 30 A/cm^2, while for high power MBKs with an average power of ~ 10 kW, practical limits on the cathode loading are ~ 15 A/cm^2.

Reference [22] reports significant progress in the development of metal-porous cathodes (MPCs) capable of operating at current densities in excess of 30 A/cm^2 for over 10^4 hours. The basic emission body is described as a "tungsten sponge" impregnated with barium calcium aluminate. Figures 6 and 7 plot the current density versus lifetime and the lifetime versus operating temperature, respectively, for a variety of MPCs with different coatings and impregnants. Thermo-electron emission is enhanced by the deposition of an ~ 0.5 μm thick film of osmium on the surface of the cathode [labeled as "MPC-Os (*l*)" in Figs. 6 and 7] and by scandium oxide or metallic scandium either impregnated into the tungsten or deposited on the surface of a metallic film deposited on the surface of the cathode ["MPC-Sc"]. Lifetime can be increased by impregnating 40% to 70% osmium deep inside the tungsten sponge ["MPC-Os (*v*)"] or by using films made of osmium and a 3% hafnium alloy ["MPC-Os+Hf (*l*)"]. The most substantial increase in lifetime and current density occurs when the emitter body is created from a "laminated sponge" in which deeper layers are enriched with an active substance ["MPC-str"]. From Figs. 6 and 7, we see that it is possible to obtain ~ 30 A/cm^2 from a porous metal cathode ["MPC-Os+Hf (*l*)"] while maintaining cathode lifetimes ~ 10^4 hours or ~10 A/cm^2 with a lifetime in excess of 10^5 hours.

Three different multiple-beam cathode structures are described in [22] and are shown schematically in Fig. 8. In Fig. 8(a), the separate cathodes and the cathode mask are kept at the same temperature. The edges of cathodes and the front face of the mask are located in the same plane; to suppress emission, the mask is covered with an anti-emission material. If there are high electric fields in the gun region, an arc breakdown could develop between the mask and either the control electrode or anode. One solution to this problem is to move the mask away from the electrodes, as shown in Fig. 8(b). To confine emission to the cathode faces, the non-emitting sides of the cathode columns are covered in anti-emission material (in addition to the surface of the mask). Finally, thermo-electron emission from the mask can be reduced by reducing the temperature of the mask and decreasing the amount of thermal contact between the mask and the cathodes, as shown in Fig. 8(c).

Ion back-bombardment is another important factor that affects the lifetime of multiple-beam cathodes. It is critical to prevent electrons from impinging on metallic surfaces such as collector surfaces or resonator drift tubes with sufficient current density so as to produce thermally-generated ions that could make their way back to the cathode emitters; the beam guiding system should ensure that the spent beamlets are homogeneously distributed over the collector surface.

There has been a substantial effort to develop depressed collectors for MBKs to enhance the overall efficiency. Depressed collector design is particularly challenging for the MBK because the high total beam current can cause the appearance of reflected electrons due to voltage depression. These reflected electrons cause parasitic excitation in MBKs and degrade the spectrum of radiation. Several techniques have been suggested to solve this problem [14], which include: op-

timizing the shape of the collector, providing individual collectors for each beamlet, and the addition of a special electrode to extract the reflected electrons.

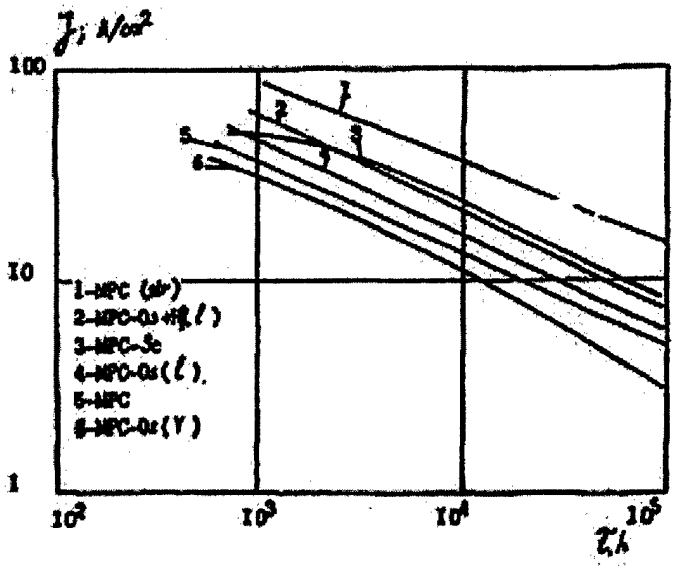

Figure 6: Cathode current density versus lifetime for a variety of metal-porous cathodes [22].

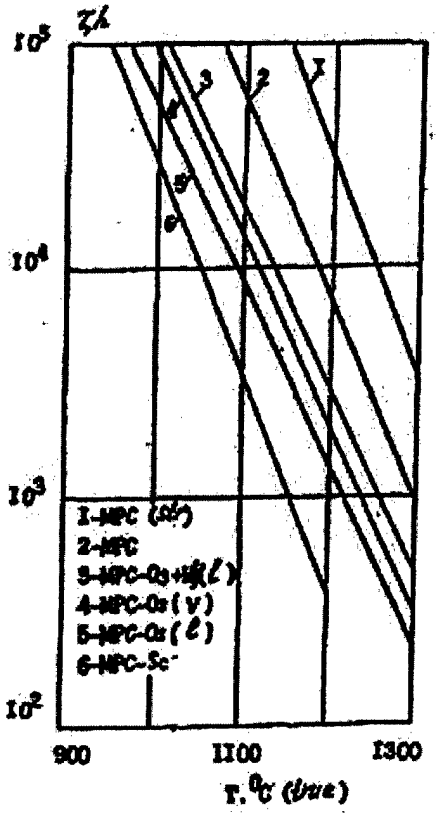

Figure 7: Cathode lifetime versus temperature for a variety of metal-porous cathodes [22].

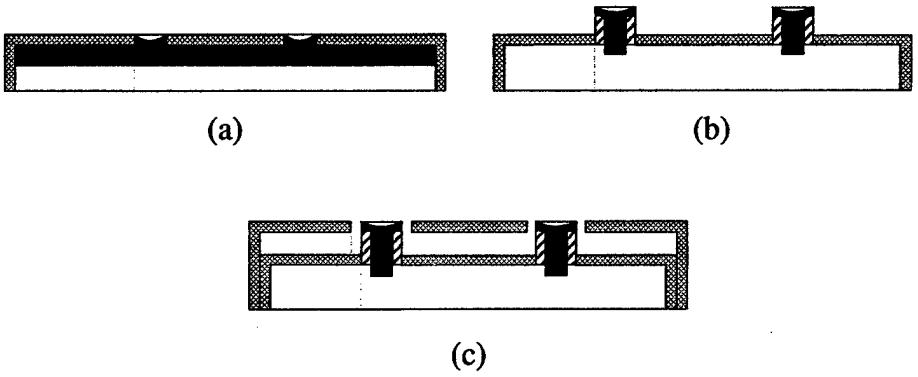

Figure 8: Examples of multiple-beam cathode structures [22].

5.2 Magnets

The presence of radial magnetic fields, which cause azimuthal rotation of the beamlets [36], is another important issue. This helical motion must be suppressed in order to provide for good beam transport [34][37][38]. As discussed in [4], the ratio of radial to axial magnetic field components, B_r/B_z, must be less than or equal to 2% to ensure 99% beam transmission without rf fields present and up to 96% with rf fields present. Other researchers suggest even more stringent requirements: for example, [20] recommends a more conservative value of $B_r/B_z = 0.2\%$.

In some cases, magnetic field uniformity is achieved by adding rings of different magnetic material around the individual beamlet drift tubes. These materials have the effect of locally "straightening out" the magnetic field produced by the global guiding magnet system [14].

Magnetic fields for MBKs have been produced with both solenoid electromagnets and by permanent magnets. Solenoids can provide a highly uniform longitudinal magnetic field, which is important for focusing beams with large longitudinal extents. According to [15], the power requirement for a solenoid magnet system is relatively low, typically $\leq 5\%$ of the beam average power. High-power MBKs usually use solenoid magnet systems. For fixed installations, such as shipboard radar and many industrial applications, the solenoid system has the advantage that it can be semi-permanently installed independent of the MBK tube – an arrangement that is convenient and cost-effective as the tube can then be removed for repair or replacement as needed, without replacing the solenoid (which can account for as much as half of the total MBK device cost). For medium- and low-power MBKs used in mobile and/or volume-/weight-constrained platforms, permanent magnet focusing is used to guide the beamlets.

5.3 Microwave circuits

A variety of resonator types can be used in MBKs. These include ring and toroidal single-gap resonators operating in the fundamental mode, and resonators operating in higher-order modes. To further increase the device bandwidth, multi-gap resonators (≥ 2 gaps) and coupled-cavity resonators have been also utilized.

The most widely-used type of resonator is the fundamental mode resonator, shown in Fig. 9. Devices using this resonator type tend to have lower magnet weights and relatively large bandwidths.

MBKs designed to operate at higher-order modes have the potential to further increase the output power while maintaining low operating voltages. Such devices were first studied in [6]. In the higher-order mode MBKs, each beamlet is placed at a peak in the rf field. It is important to remember that higher-order modes do not provide as much bandwidth as would be attained if all the current passed through the field maximum of a fundamental mode. If higher-order mode circuits are used, the bandwidth will be lower, approaching the bandwidth of a single-beam klystron driven with a single MBK beamlet. In other words, the MBK will act like a collection of low-power klystrons operated in parallel. Examples of higher-order mode resonators are shown in Figs. 10 and 11. One can view such higher-order mode MBKs as a collection of many single-beam klystrons using a common electron gun, vacuum envelope, magnetic field, and rf cavities. There are MBKs that consist solely of a common vacuum envelope and common magnetic field. Such an MBK configuration (in *W*-band) is currently under consideration at the Stanford Linear Accelerator Center and has been termed a "klystrino" [39].

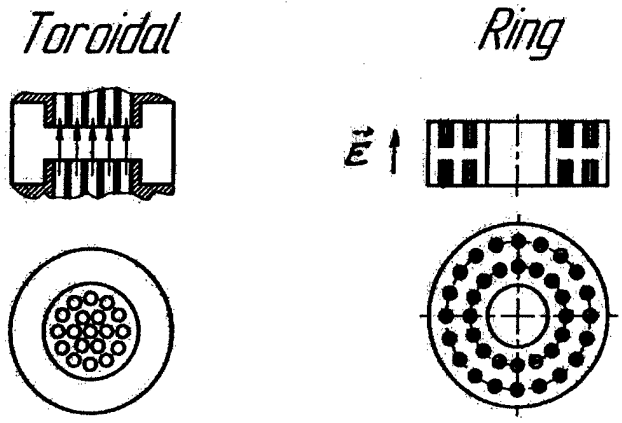

Figure 9: Toroidal and ring single-gap fundamental-mode resonators [18].

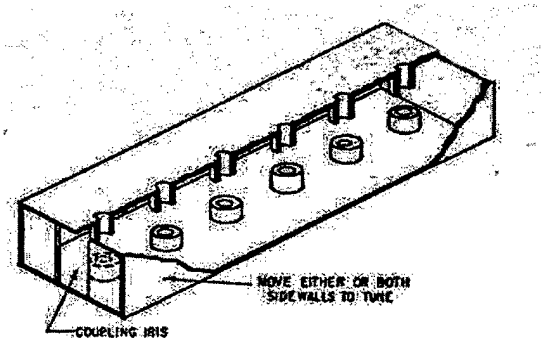

Figure 10: Distributed beam resonator [6].

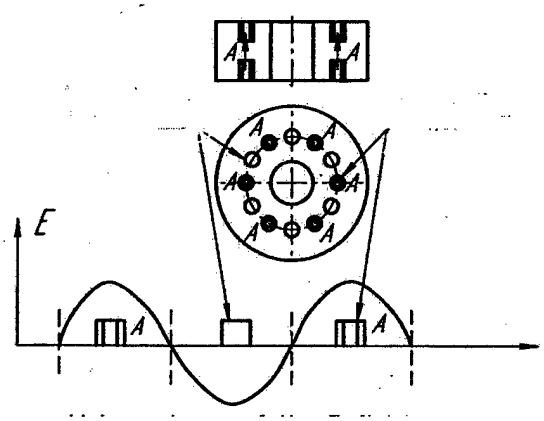

Figure 11: Resonator operating in higher-order modes [18].

To enhance both the power and the bandwidth, a hybrid approach has been employed [18]. The hybrid approach combines elements of fundamental mode and higher-order mode devices. As in the higher-order mode devices, the hybrid device uses multiple channels to place the beam electrons at the peaks of the higher-order mode electric field. The difference in the hybrid device, however, is that instead of a single beam in each channel, there are multiple, parallel beamlets, as shown in Fig. 12. In [18], this configuration is termed a "multiple-stem"-like klystron where each individual stem acts like an MBK operating in the fundamental mode of the resonator. Referring to Fig. 12, the tube, whose resonator cross-section is shown on the left, demonstrated a peak power of 200 kW (15 kW average) with a bandwidth of > 2% in *X*-band; this particular tube used a total of 54 beamlets.

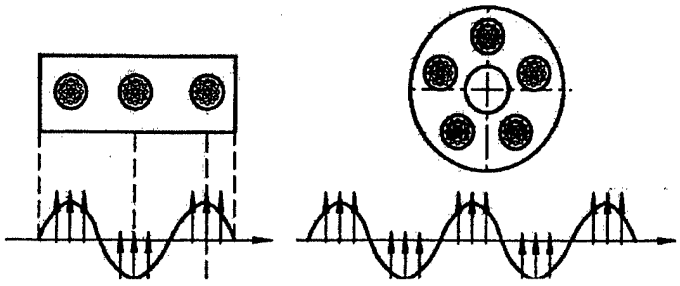

Figure 12: Hybrid MBK resonator and beam structures tested at "Istok" [18].

Coupled-cavity and multi-gap resonators used in MBKs are described in [14] and [17]. These structures are very similar to those used in conventional SBKs except that in the case of MBKs, the resonators have N holes to accommodate the N beamlets. In the end, the optimum choice of the type of resonator depends on the requirements of the particular application, *e.g.*, wavelength, bandwidth, peak and average power, *etc.* There is an interesting note in [4] stating that an optimal spacing between gaps in multi-gap resonators reduces the sensitivity of operation to voltage fluctuations. Finally, traveling-wave rf structures, such as coupled-cavity TWTs, have been successfully used in multiple-beam devices; Fig. 13 is an example of such a structure. Section 7 describes multiple-beam TWTs in greater detail.

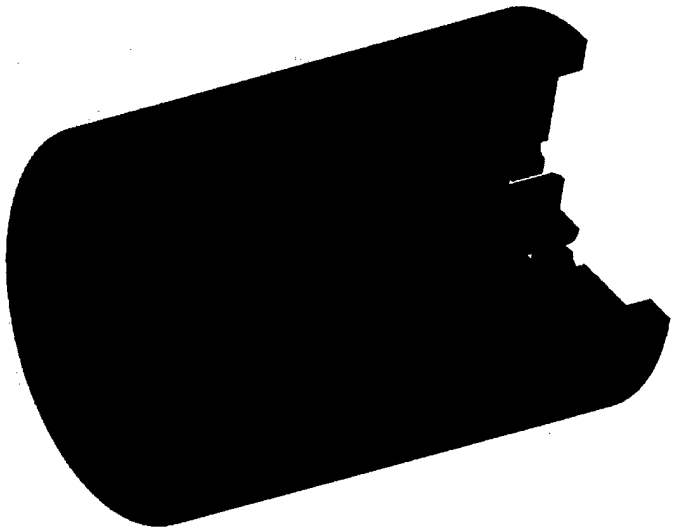

Figure 13: Example of a coupled-cavity TWT structure for use with multiple electron beams.

5.4 Fabrication and alignment

The mechanical dimensions of an MBK operating in the fundamental mode are proportional to the wavelength of operation. At microwave frequencies, the fabrication of MBKs is relatively easy. However, as the wavelengths get shorter, the requirements for alignment precision and manufacturing tolerances become increasingly stringent; millimeter-wave MBKs represent a potentially significant manufacturing challenge. The use of higher-order mode designs for millimeter-wave MBKs could reduce some of the fabrication difficulties.

Despite manufacturing challenges, however, MBKs have been successfully developed for applications in *L*-, *S*-, *X*-, and K_u-bands. The current status of MBK development in the Russia Federation, France, and the PRC is presented in the following section. We should also mention the progress in manufacturing the elements of a *W*-band MBK (*i.e.*, the "klystrino") demonstrated at SLAC [39] by using a new technology called LIGA (the German acronym for Lithographie-Galvanoformung-Abformung, a micro-electro-mechanical manufacturing technique that uses synchrotron x-ray radiation to expose patterns in cast acrylic resists). This technology enables parts to be fabricated with better than 1 μm resolution.

6 STATE-OF-THE-ART

In Russia, three companies – "Istok", "Toriy", and "Svetlana" – have been involved in the development of MBKs for several decades. These companies, according to [29], have developed several tens of types of MBKs, possibly more. Information about the MBK work at "Istok" is documented in [13]-[19] and the activities at "Svetlana" are reviewed in [4]; there is little available information about the MBK work at "Toriy".

Following [4][19], it is convenient to divide MBK types into three categories: high-power, medium-power, and low-power miniaturized MBKs.

6.1 High-power MBKs

Table 1 summarizes the parameters of some high-power MBKs developed at "Istok" for radar applications [16][17][19]. The gains of all of the tubes in Table 1 are in the range of 40 to 45 dB.

The column for MBK model 213-1 in Table 1 summarizes the parameters in the MBK operating in a higher-order mode; all other columns contain data for devices operating in the fundamental mode. Note that the current density in the higher-order mode MBK is much lower compared to the fundamental-mode tubes, and is presumably responsible for the greatly increased lifetime of the device (on the other hand, its bandwidth is much lower). A schematic of the cavity used in this tube is shown on the left in Fig. 9. Photographs of two high-power MBKs are shown in Fig. 14. The left-hand photograph is of MBK model 214-1 and the right-hand photograph is of MBK model 213-1 (see Table 1 for specifications).

Table 1: High-power MBKs for radar [4][19].

Parameter	Model 213-1[++]	Model 214-10	Model 214-4	Model 214-3	Model 214-2	Model 214-1
Wavelength (cm)	3	3	5.5	7	10	15
Peak supplied power (kW)	570	400	700	1100	1650	2010
Cathode voltage (kV)	26	24	24	29	31	32
Control voltage (kV)	5.5	5	4.5	6	6	5.7
$P_{out,\,peak}$ (kW)	200	120	220	500	600	800
$P_{out,\,average}$ (kW)	17	3	11	17	12	14
$\Delta f / f$ (%)	0.7	2	3.5	4.5	6.5	10
Number of beams	6	15	24	24	36	36
Weight* (kg)	12	10	20	20	25	32
Emitter loading (A/cm^2)	2.5	21	13	16	11.6	11
Perveance per beam (microperv)	0.87	0.3	0.33	0.32	0.27	0.3
Total perveance (microperv)	5.2	4.5	8	7.7	9.8	11

*without magnet.

[++]higher-order-mode resonators.

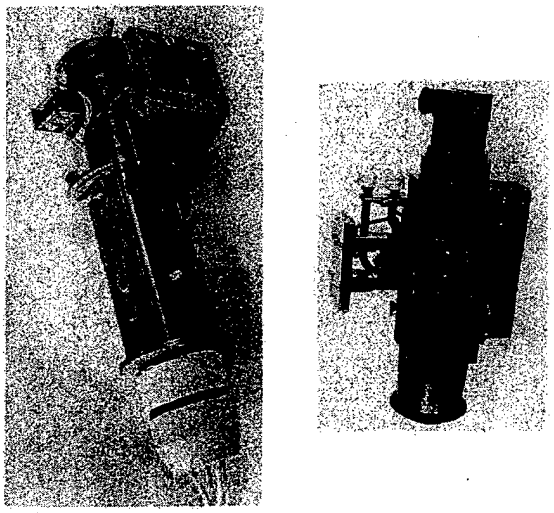

Fundamental mode resonator
f_{op}=2GHz, Pav=14kW
P_{puls}=800kW
Cathode voltage 32kV
Δf=10%

High mode resonator
f_{op}=9GHz, Pav=17kW
P_{puls}=200kW
Cathode voltage 26kV
Δf=0.7%

Figure 14: High-power MBKs [17].

Reference [4] reports on the development of a 61-beamlet MBK, which delivers about 7 kW peak power with an 18%-bandwidth at wavelength larger than 10 cm. To date, this is the maximum number of beamlets used in MBKs that has been reported in the open literature. The number is consistent with the estimate made in [6]: "... the best present estimate for typical existing klystrons is that the limitation will occur somewhere between 40 and 100 beams." More typically, the number of beamlets is equal to 7, 19 or 37; the beamlet packing structure is: one beam in the center, six beams around it, twelve beams around the six, etc. In some cases the center beam is removed, as is reported in [21], because it is most strongly affected by voltage depression.

6.2 Medium-power MBKs

Medium-power MBKs are typically designed to operate in *C*- to K_u-bands (5 to 15 GHz). Their peak powers range from 10 to 70 kW with bandwidths typically in the range of 2% to 6%. The main parameters of several medium-power wide bandwidth MBKs are listed in Table 2 [19]. Typically, these tubes exhibit a very flat power versus frequency response within their several percent bandwidths.

Table 2: Broadband medium-power MBKs [19].

Parameter	K_u-band	X-band	X-band
$P_{out,\,peak}$ (kW)	≥ 25	≥ 25	70
$P_{out,\,average}$ (kW)	1.5	3	3.5
1-dB bandwidth (%)	2	6	6
Electronic efficiency (%)	≥ 35	≥ 35	~ 40
Gain (dB)	≥ 40	≥ 40	~ 45
Cathode voltage (kV)	14	11	13
Control voltage (kV)	3.8	2.5	3.5
Number of beams	15	24	24
Perveance (microperv)			
total	3.8	8.3	5.6
per beam	0.25	0.34	0.23
Output circuit	two-gap	three-gap	three-gap
Power output system	3 coupled-cavity	3 coupled-cavity	3 coupled-cavity
Magnetic focusing	permanent magnet	permanent magnet	permanent magnet
Weight (kg) (including magnet)	8	16	16

6.3 Low-power, miniaturized MBKs

Low-power, miniaturized MBKs (MMBKs) have been developed for a variety of volume- and weight-constrained applications. In addition to meeting performance specifications such as power, efficiency, gain and bandwidth, these tubes must also meet quite severe limitations on weight and volume, cathode and control voltages, and cooling. The main parameters of some of the MMBKs developed at "Istok" are listed in Table 3. Note that all the tubes, whose parameters are listed in this table, operate at relatively high cathode current densities ranging from 15 to 25 A/cm^2.

Table 3: Low-power miniaturized MBKs [19].

No.	f_0 (GHz)	$P_{out,\,pk}$ (W)	Δf (MHz)	Gain (dB)	Duty cycle	V_b (kV)	$V_{control}$ (V)	No. of beams	η (%)	Wt.* (kg)
1	17	400	40	47	0.33	2.5	500	18	30	1.0
2	17	1000	100	40	0.05	3.5	1000	19	30	1.2
3	15	400	40	40	0.33	2.5	500	18	30	0.4
4	16	500	200	37	0.04	3.5	1000	19	25	1.2
5	14	400	60	40	0.33	2.5	500	18	30	1.0
6	9.3	1000	60	40	0.04	3.5	anode	19	35	1.5
7	9	50	180	37	0.04	1.5	anode	19	12	1.2

*Including the magnet.

Photographs of two of these tubes are shown in Fig. 15. One of the most remarkable tubes is the Tube #3 in Table 3. The tube delivers 400 W peak power with a >30% duty-cycle while weighing only 400 g, including the magnet (an impressive peak-power-to-weight ratio of 1 Watt/g). One of these tubes was used in the Russian space station "Mir".

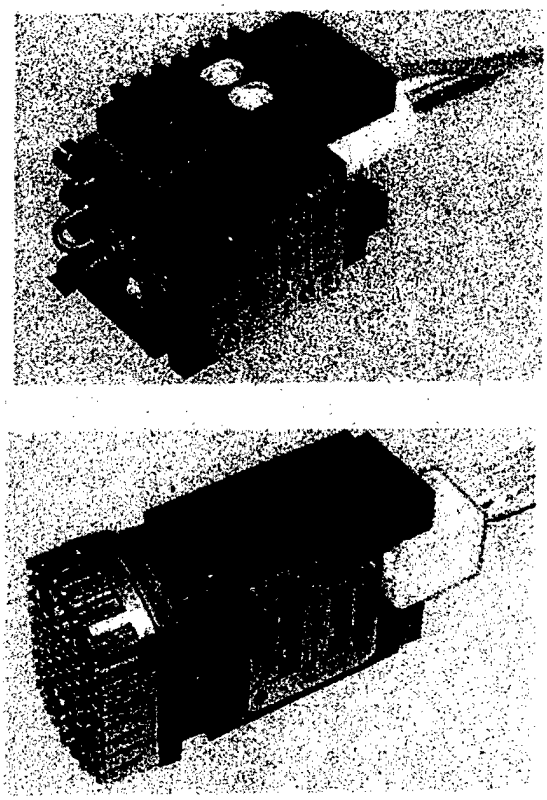

Figure 15: Low-power miniaturized MBKs [17].

6.4 MBK development at "Svetlana" [40]

MBKs have been under development at "Svetlana" since 1958. The company currently manufactures more than 20 types of MBKs and is actively developing several types of MBKs for radar and communications applications. The parameters for an older model "Svetlana" CW *L-/S*-band SBK (SBK-66) and MBK (MBK-68) are shown in Table 4 columns (the numbers 66 and 68 apparently correspond to the year of development). For comparison purposes, the parameters of a similar U.S.-built SBK (Litton L-3910B) are also shown in Table 4. As can be seen in the table, the MBK has a significantly higher gain, larger bandwidth, and lower operating voltage than either of the SBK tubes.

Pulsed *X*-band MBKs followed the development of the *L-/S*-band MBKs. The parameters of two *X*-band tubes, MBK-88 and MBK-98, are shown in Table 5; as in Table 4, the parameters of a similar U.S.-built SBK (CPI VA-956) are included for the purposes of comparison. Again, MBKs demonstrate much larger instantaneous bandwidth while operating at much lower voltages. For "Svetlana" model MBK-98, the peak-power-to-weight ratio is in excess of 4 Watts/g (although it is not clear whether the weight listed in Table 5 includes the magnet).

Table 4: Comparison of an *LS*-band, CW MBK [40] developed by "Svetlana" with a Litton SBK and a Russian SBK.

Parameters	L-3910B	SBK-66	MBK-68
Center frequency (MHz)	2287	2287	2250
Output power (W CW)	20	20	30
Gain (dB)	20	40	60
Instantaneous bandwidth (MHz)	4	10	60
Cathode voltage (V)	1600	1500	650
Total beam current (mA)	50	50	180
Weight (kg)	1.18	1.18	1.36

Table 5: Comparison of pulsed, *X*-band MBKs [40] developed by "Svetlana" with a Varian SBK.

Parameters	VA-956	MBK-88	MBK-98
Center frequency (GHz)	9.25	9.25	9.25
Output power (kW peak)	7.5	6	50
Gain (dB)	45	43	43
Instantaneous bandwidth (MHz)	45	500	500
Cathode voltage (kV)	13.5	5	5
Total beam current (A)	1.6	4	40
Weight (kg)	22.7	7.3	11.3

6.5 MBK Development in France

In France, several high-power, low-frequency MBKs have been developed by Thales Electron Devices, primarily for accelerator applications. Thales designers cite the relatively low voltage operation of the MBK and its relatively high R/Q as the principle attractions of the technology [20]. Lower voltage is desirable as, in general, it leads more compact packaging, lower cost, increased reliability, and reduced high voltage and x-ray hazards. In addition, the probability of dc breakdown is reduced by more than 50% to 60% in an MBK compared to an SBK of comparable power, opening up possibilities for longer pulse lengths [20]. The higher R/Q's possible with MBK circuits lead to higher instantaneous bandwidths.

The parameters of selected Thales tubes are listed in Table 6. These data again demonstrate that MBKs, in comparison with SBKs of equivalent output power, can operate at much lower voltages and have much smaller weights and volumes. In Table 6, the bandwidth is not shown since this is not a critical parameter for accelerator applications. Note that the number of beamlets in tubes whose parameters are shown in Table 6 is equal to 6 or 7. Also, in Table 6, all data correspond to designs intended for CW operation.

Parameters of existing tubes are given in the first and third columns of Table 7, taken from [36]. Recently, Thales Electron Devices has developed a 7-beam MBK producing 10 MW peak, 0.4 millisecond duration pulses at 1.3 GHz for accelerator applications [20]. Also, Thales has developed a 1 MW, 4%-bandwidth, pulsed, *S*-band MBK.

Table 6: High-power SBK and MBKs (tentative) developed at Thales Electron Devices, France .

Parameters	Klystron	MBK	MBK	MBK	MBK
Center frequency (MHz)	352	425	850	850	1700
Output power (kW CW)	1300	1000	500	1000	850
Cathode voltage (kV)	100	30	30	38.5	40
Total beam current	20	7 × 5.7 A	7 × 4.17 A	6 × 6.5 A	6 × 6.4 A
Drift tube radius (mm)	36	20	8.8	10	6
Electronic efficiency (%)	65	65	58	58	56
Gain (dB) / drive power (W)	42 dB/80 W	45 dB/30 W	45 dB/15 W	45 dB/30 W	42 dB/50 W
Emitter loading (A/cm^2)	0.6	1.1	2.1	2.6	4.7
Body length (m)	2.65	1.60	0.85	0.90	0.55
Collector length (m)	1.35	0.95	0.75	0.95	0.95
Electron gun length (m)	0.751	0.35	0.25	0.35	0.35
Electron gun insulation	oil	air	air	air	air
Overall length (m)	4.75	2.9	1.85	2.20	1.85
Overall diameter (m) (including magnet)	0.90	0.58	0.36	0.36	0.34
Overall weight (kg) (including magnet)	2150	650	460	580	450
Magnetic induction (G)	270	320	650	650	900
Output waveguide	WR2300	WR1800	WR975	WR975	WR430
Output-power-to-mass ratio (W/g)	0.60	1.54	1.08	1.72	1.78

Table 7: Example of MBKs developed at Thales Electron Devices, France.

Parameter	MBK	MBK	MBK	SBK
Device status	(in operation)	(design)	(in operation)	TH 2105
Center frequency (MHz)	425	500	850	508
Output power (kW, CW)	100	1000	500	1000
Cathode voltage (kV)	17	39	33	90
Total beam current	6×1.8 A	6×6.8 A	6×4.8 A	18.5 A
Input power (W)	6	100	50	100
Gain (dB)	42	40	40	40
Electronic efficiency (%)	55	64	53	62
Number of cavities	4	5	4	5
Electron gun insulation	air	air	air	oil
Total length (m)	1.35	2.50	1.85	4.50
Weight* (kg)	400	800	600	1700

*including focusing solenoids

6.6 MBK development in the PRC

To date, more than 20 varieties of MBKs have been developed in the PRC [21][23][27][28]. The performance specifications and test results for some of these tubes are tabulated in Tables 8a and 8b, respectively. In addition to the tubes listed in Table 8, which were developed for radar and communication systems, a 5 MW, short-pulse, S-band MBK has been developed for accelerator applications [27].

Table 8: Specification and test results for MBKs developed at the Institute of Electronics, Beijing, PRC [27][28].

Table 8a: Performance specifications of selected MBKs.

Model	Band	$P_{out,peak}$ (kW)	$\Delta f / f$ (%)
KS-57	S	200	8
KS-60	*S*	200	7
KS-72	*S*	180	8.4
KC-67	*C*	50	1.75
KX–79	*C*	150	5.2
KL-81	*L*	180	11.2

Table 8b: Test results for selected MBKs.

Model	V_b (kV)	I_{total} (A)	$P_{out,peak}$ (kW)	η (%)	$\Delta f / f$ (%)	W (kg)
KS-57	18.6	32.4	263	43.6	9.1	47
KS-60	18.8	22.4	184	43.7	7.6	43
KS-72	17.1	28.8	200	39.2	8.4	45
KC-60	17.8	10.0	72	40.4	2.4	35
KL-81	18-19	-	140	-	10.8	-

7 MULTIPLE-BEAM TRAVELING-WAVE TUBES

Advances in the development of MBKs have been applied to the development of low-voltage, multiple-beam traveling-wave tubes (MBTWTs). In the late 1970s, such multiple-beam coupled-cavity TWTs were developed at "Istok" [14]. Initially, the multiple beam was focused by a built-in solenoid, making the system (tube plus solenoid and solenoid power supply) heavy. Later, this single-tube system was replaced by a chain of tubes consisting of a pre-amplifying, single-beam, multi-stage, high-gain, helix TWT followed by a multiple-beam, single-stage, low-gain (13 dB), high-efficiency (30-35%), coupled-cavity TWT [14][41]. The short length of this MBTWT allowed developers to use permanent magnets for beam focusing, drastically reducing system weight and volume. Since multiple-beam devices can operate at low voltage, the operating voltage of this MBTWT was chosen to be equal to the operating voltage of the single-beam TWT pre-amplifier, with the advantage that the same high-voltage supply could be used for both tubes. The performance and operating parameters of the *X*-band helix TWT pre-amplifier plus 36-beam MBTWT output amplifier chain are given in Table 9.

Table 9: Parameters of the helix TWT pre-amplifier, MBTWT output stage, and the overall system (helix TWT + MBTWT) [14][41].

Parameters	Helix TWT pre-amplifier	36-beam MBTWT
Bandwidth (GHz)	0.6	0.6
Cathode voltage (kV)	8.4	8.4
Max. $P_{out,\,peak}$ (kW)	0.4	5
Range of realizable output powers thru variation of the MBTWT beam current (kW)	—	0.4 – 5
Gain (dB)	47	13
Electronic efficiency (%)	—	30-35
Magnet system type	PPM	permanent magnet
Weight* (kg)	1.5	6

*Including the magnet.

As can be seen in Table 9, the amplifier chain has an overall gain of 60 dB. Note that, similar to a crossed-field amplifier (CFA), the MBTWT is a "pass-through" device since there is no attenuation in the microwave circuit. In other words, the amplifier chain will operate even with the MBTWT turned-off. In this mode, the MBTWT output stage of the chain operates as a waveguide with a relatively small (0.5 dB) insertion loss and the system amplifying characteristics are determined solely by the TWT pre-amplifier. Such a wide range of power levels allows

one to use these tubes in satellite communication systems where the power level should correspond to a variable number of users or where the variable power could be used to compensate for weather/atmospheric effects. Another important feature of the MBTWT is the almost linear dependence of its output power on the beam current, which allows one to vary the power by as much as 5 dB while maintaining an electronic efficiency of about 35%. All these features provide a wide dynamic range of output power without the need for specialized tuning of the operating voltage and/or input power.

Before closing this section, we will also note that in [17], the development of electrostatically-focused multi-beam backward-wave oscillators operating at frequencies up to 40 GHz was briefly mentioned.

8 CONCLUSIONS

The current state-of-the-art in multiple-beam device design and manufacturing has a demonstrated high level of sophistication and precision, successfully overcoming issues of increased device complexity. At present, various types of multiple-beam klystrons have been developed for radar, telecommunications, and high-energy particle accelerator applications; many of these tubes are in every-day use. These applications have clearly demonstrated the technology's advantages which include low-voltage operation (two to three times lower than that required for SBKs operating at the same output power level); high electronic efficiency (up to 65%) due to the mitigation of space charge effects; low magnet system weight (up to ten times lower than in an equivalent SBK); reduced overall system weight and volume; large bandwidth; low phase sensitivity to voltage deviations; and reduced x-ray generation. The availability of advanced, physics-based computational tools for 3D electron gun and collector design, coupled with advances in manufacturing technology and high current density cathodes are critical enabling technologies that are providing a new impetus for MBK development in the U.S.

In conclusion, it is worth highlighting some operational advantages of using MBK technology, for example, (1) MBKs, like other linear-beam devices (*e.g.*, SBKs and TWTs), have a much larger dynamic range than CFAs, making them attractive for use in radar and communication systems that require complex waveforms; (2) since MBKs have lower operating voltages and shorter circuit lengths than SBKs of comparable power, the close-to-carrier noise is reduced in the MBK, making them preferable for noise-sensitive applications; (3) MBKs have a high output-power-to-weight ratio (two to three times higher than that of an equivalent SBK), an important feature for weight- and volume-constrained platforms; (4) MBKs are capable of higher peak and average power levels in comparison with TWTs; and (5) MBKs are less sensitive to vibrations in comparison with TWTs.

This memo is motivated by our wish to understand the current state-of-the-art in multiple-beam technology. It is based on open-literature materials that have been collected and analyzed over a two-year time period (2000-2002), drawing primarily on publications and presentations from researchers in the Russian Federation, France, and the People's Republic of China. We acknowledge that the memo does not refer to all available material, but nevertheless, we hope that it accurately presents the present status of the development of multiple-beam amplifiers.

9 ACKNOWLEDGEMENTS

The authors are greatly indebted to E. Gelvich, R. Symons, G. Caryotakis, A. Staprans, and B. James for useful discussions. This work was supported by the U.S. Office of Naval Research.

10 REFERENCES

[1] V.F. Kovalenko, A.S. 72756, USSR, kl. 21, 1940.

[2] J. Bernier, Pat. 992853, (France) Multiple beam device, 1944.

[3] S.A. Zusmanovsky, A.S. 155556, USSR, 1955.

[4] E.A. Gelvich, L.M. Borisov, Y.V. Zhary, A.D. Zakurdayev, A.S. Pobedonostsev, and V.I. Pugnin, "The new generation of high-power multiple-beam klystrons," *IEEE-MTT*, vol. 41, no. 1, pp. 15-19, January 1993.

[5] Thales Electron Devices, France. [Online]. Available WWW: http://www.thales-electrondevices.com/jrun_tte/Products_us/science/t037.jsp, 2002.

[6] M.R. Boyd, R.A. Dehn, J.S. Hickey, and T.G. Mihran, "The multiple-beam klystron," *IRE-ED*, vol. 9, pp. 247-252, 1962.

[7] A. Staprans, E.W. McCune, and J.A. Ruetz, "High-power linear-beam tubes," *Proc. IEEE*, vol. 61, no. 3, pp. 299-330, March 1973.

[8] R. Symons, private communication, 2002. (The high voltage equipment that had been used to design and test components for the 238 kV Hoover Dam-to-Los Angeles transmission line was available at Stanford University and was used by M. Chodorow and E. Ginzton to conduct early tests on the Stanford Linear Accelerator klystron.)

[9] R. Symons, private communication, 2002.

[10] A. Staprans, private communication, 2002.

[11] L. Falce, private communication, 2002.

[12] *TriService/NASA Cathode Life Test Facility Annual Report, January 2001-March 2002*, Naval Surface Warfare Center, Crane Division, Crane, IN, March 2002.

[13] E.A. Gelvich, L.M. Borisov, E.V. Zhara, A.D. Zakurdayev, A.S. Pobedonostzev, and V.I. Pugnin, "A new generation of high power multi-beam klystron," *IEEE MTT-S International Microwave Symposium Digest*, vol. 3, 1991.

[14] L.M. Borisov, *et al.*, "High-power multi-beam vacuum microwave amplifiers," *Elektron. Tekhnika*, Ser. 1, Elektron. SVCh, No. 1, pp. 12-20, 1993 (in Russian).

[15] E.A. Gelvich and M.I. Lopin, "New generation of microwave amplifiers of high and average power," *Radiotekhnika*, No. 4, pp. 18-31, 1999 (in Russian).

[16] E.A. Gelvich "The trends in the development of high power amplifiers and oscillators of electromagnetic radiation at UFH in Russia," *Electron. Technika*, ser. SVCh, #1, pp. 27-41, 1995 (in Russian).

[17] A. Pobedonostsev, A. Korolyov, S. Zaitsev, I. Golenitskij, E. Zhary, A. Zakurdayev, M. Lopin, P. Meleshkevich, A. Negirev, V. Poognin, and V. Homich, "Traditional and novel areas of vacuum electronics in SRPC Istok," oral presentation, *1st IEEE Int. Vacuum Electronics Conference*, Monterey, CA, May 2-4, 2000.

[18] E.A. Gelvich, "Multi-beam klystrons, trends in the development (review)", invited talk given at the Workshop "Multiple Beam Amplifiers: Current Status and Future Trends," SAIC, McLean, VA, May 18, 2001.

[19] E.A. Gelvich, E.V. Zhara, A.D. Zakurdayev and V.I. Pugnin "Multi-beam klystrons, trends in the development," in *Vacuum Microwave Electronics*, Ed. M.I. Petelin, Institute of Applied Physics, Russian Academy of Sciences, Nizhniy Novgorod, Russia, 2002 (in Russian).

[20] C. Bearzatto, A. Beunas and G. Faillon, "Long pulse and large bandwidth multibeam klystron," *RF-98 Workshop*, Pajaro Dunes, CA, Oct. 1998; "High Energy Density Microwaves," Ed. R.M. Phillips, *AIP Conf. Proc.* 474, Woodbury, New York, 1999, pp. 107-116.

[21] D. Yaogen, "Recent progress on L-band broadband MBK," *3rd IEEE Int. Vacuum Electronics Conference*, Conference Digest, pp. 296-297, April 22-25, 2002, Monterey, CA.

[22] B. Ch. Djubua, O.V. Polivnikova, N.M. Ogoleva, Y. Ding, and J. Peng, "The impregnated cathode for high power klystrons," *Proc. of the 2nd Int. Conf on Microwave and Millimeter Wave Technology*, Beijing, PRC, September 14-16, 2000.

[23] D. Yaogen, X. Xianghui, V.E. Rodiakin, and A.N. Sandalov, "Theoretical and experimental investigations of high power MBK based on 2.5D Arsenal-MSU computer code," *Proc. of the 2nd Int. Conf. on Microwave and Millimeter Wave Technology*, September 14-16, 2000, Beijing, PRC.

[24] G.M. Branch and T.G. Mihran, "Plasma frequency reduction factors in electron beams," *IRE Trans. on Electron Dev.*, vol. ED-2, pp. 3-11, April 1955.

[25] M. Chodorow and C. Susskind, *Fundamentals of Microwave Electronics*, New York: McGraw-Hill Book Co., 1964.

[26] S.V. Korolev, "On one possibility to reduce weight and sizes of transit klystrons," *Elektron. Tekhnika*, Ser. 1, Elektron. SVCh, No. 9, pp.176-178, 1968, (in Russian).

[27] D. Yaogen, *et al.*, "Theoretical and experimental research on multi-beam klystrons," seminar at the Institute for Plasma Research, University of Maryland, Oct. 15, 1998.

[28] D. Yaogen, "Recent progress in multi-beam klystron in IECAS," *High Energy Density and High Power RF*, 5th Workshop on High Energy Density and High Power RF, B.E. Carlsten, ed., pp. 29-33, Snowbird, Utah, October 1-5, 2001.

[29] E.A. Gelvich, "Multiple beam klystrons and traveling wave tubes exclude or complement each other?," *Radiotechnika*, no. 8, pp. 21-29, 2002.

[30] V. I. Poognin, "Estimates for utmost power capabilities of multiple-beam klystrons with cavities operating at fundamental mode for radar applications," *Radiotechnika*, no. 2, pp. 43-50, 2000.

[31] A.Z. Khaikov, *Klystron Amplifiers*, Sviaz, Moscow, 1995, (in Russian).

[32] A.S. Pobedonostsev, *et al.*, "Multiple-beam microwave tubes," paper presented at the *RF-98 Workshop*, Pajaro Dunes, CA, Oct. 1998.

[33] R.S. Symons, "Multiple-beam klystrons for radar and communications applications," private communication, 1999.

[34] K. Nguyen, D. Pershing, J. Pasour, and J. Petillo, "Multiple beam electron gun development for high-power amplifiers," *3rd IEEE Int. Vacuum Electronics Conference*, Monterey, CA, April 23-25, 2002, 02EX524, p.168.

[35] R.L. Ives, *et al.*, "Confined flow multiple beam guns for high power rf applications," presentation at the Workshop "Multiple Beam Amplifiers: Current Status and Future Trends," SAIC, McLean, VA, May 18, 2001.

[36] G. Faillon, "Sources hyperfrequences de grande poissance," *Revue Technique Thomson-CSF* 23, pp. 795-830, 1991.

[37] L. Ives, G. Miram, M. Mizuhara, D. Marsden, A. Krasnykh, and V. Ivanov, "Confined flow multiple beam guns for high power rf applications," *3rd IEEE Int. Vacuum Electronics Conference*, Monterey, CA, April 23-25, 2002, 02EX524, p. 170.

[38] L. Ives, G. Miram, M. Mizuhara, D. Marsden, A. Krasnykh, and V. Ivanov, "Multiple beam guns for high power rf applications," *27th IEEE International Conference on Infrared and Millimeter Waves*, San Diego, CA, September 22-26, 2002, p. 103.

[39] G. Scheitrum, *et al.*, "Design and fabrication of a 94 GHz klystron," *9th Workshop on Advanced Accelerator Concepts, AIP Conf. Proc.*, vol. 569, Santa Fe, NM, June 10-16, 2000, pp. 712-724.

[40] Y. Besov, "Multiple-beam klystrons," *RF-98 Workshop*, Pajaro Dunes, CA, Oct. 1998; "High Energy Density Microwaves," Ed. R.M. Phillips, *AIP Conf. Proc.* 474, Woodbury, New York, 1999, pp. 91-106.

[41] M.I. Lopin, A.S. Podebonostsev, and B.V. Sazonov, "High-power multiple beam TWTs and the TWT-based amplifying chains," *MTT-S Conf. Digest*, pp. 145-146, 1992.